The hairpin conformation of the Amyloid β peptide is a common structural motif along the aggregation pathway

Abelein, A.; Abrahams, J.P.; Danielsson, J.; Gräslund, A.; Jarvet, J.; Luo, J.; ... ; Wärmländer, S.K.T.S.

MINIREVIEW

The hairpin conformation of the amyloid β peptide is an important structural motif along the aggregation pathway

Axel Abelein · Jan Pieter Abrahams · Jens Danielsson ·
Astrid Gräslund · Jüri Jarvet · Jinghui Luo · Ann Tiiman ·
Sebastian K. T. S. Wärmländer

Abstract The amyloid β (Aβ) peptides are 39–42 residue-long peptides found in the senile plaques in the brains of Alzheimer's disease (AD) patients. These peptides self-aggregate in aqueous solution, going from soluble and mainly unstructured monomers to insoluble ordered fibrils. The aggregation process(es) are strongly influenced by environmental conditions. Several lines of evidence indicate that the neurotoxic species are the intermediate oligomeric states appearing along the aggregation pathways. This minireview summarizes recent findings, mainly based on solution and solid-state NMR experiments and electron microscopy, which investigate the molecular structures and characteristics of the Aβ peptides at different stages along the aggregation pathways. We conclude that a hairpin-like conformation constitutes a common motif for the Aβ peptides in most of the described structures. There are certain variations in different hairpin conformations, for example regarding H-bonding partners, which could be one reason for the molecular heterogeneity observed in the aggregated systems. Interacting hairpins are the building blocks of the insoluble fibrils, again with variations in how hairpins are organized in the cross-section of the fibril, perpendicular to the fibril axis. The secondary structure propensities can be seen already in peptide monomers in solution. Unfortunately, detailed structural information about the intermediate oligomeric states is presently not available. In the review, special attention is given to metal ion interactions, particularly the binding constants and ligand structures of Aβ complexes with Cu(II) and Zn(II), since these ions affect the aggregation process(es) and are considered to be involved in the molecular mechanisms underlying AD pathology.

Keywords Alzheimer's disease · Amyloid β peptide · Hairpin · Protein aggregation · Neurotoxicity

A. Abelein · J. Danielsson (✉) · A. Gräslund (✉) · J. Jarvet ·
A. Tiiman · S. K. T. S. Wärmländer
Department of Biochemistry and Biophysics, Arrhenius
Laboratories, Stockholm University, 106 91 Stockholm, Sweden
e-mail: jensd@dbb.su.se

A. Gräslund
e-mail: astrid@dbb.su.se

J. P. Abrahams · J. Luo
Gorlaeus Laboratory, Leiden Institute of Chemistry, Leiden
University, 2300 RA Leiden, The Netherlands

J. Jarvet
The National Institute of Chemical Physics and Biophysics,
Akadeemia tee 23, 12618 Tallinn, Estonia

Introduction

Amyloid is an old term describing the solid starch-like deposits observed in the senile plaques in the brains of Alzheimer's disease (AD) patients. More recent biochemical work (reviewed in [1, 2]) has identified the major plaque component to be Amyloid β (Aβ) peptides. These peptides are relatively short, typically 39–42 residues long, and are formed by enzymatic processing from the amyloid precursor protein (APP). The amyloid deposits contain relatively regular fibrillar structures, which can be visualized by e.g., electron microscopy (EM).

From a biophysical/structural perspective, amyloid material may be defined by a characteristic pattern in X-ray fiber diffraction measurements. There is a common structural motif in these fibers, which is named "cross-β structure", that gives rise to 4.7 Å meridional and 10 Å equatorial reflexions in the diffraction pattern [3, 4]. The structure

consists of repeating units of peptide (protein) segments which are positioned perpendicular to the fiber (fibril, describing a very thin fiber) axis. The "cross-β structure" arises when β-sheets are formed with intermolecular H-bonds aligned along the fibril axis. In mature fibrils, the β-sheets are generally in register and parallel to each other. The Aβ peptides are one of several kinds of amyloid-forming peptides/proteins associated with human neurodegenerative disorders. Other examples are α-synuclein, associated with Parkinson's disease, superoxide dismutase 1 (SOD1), associated with amyotrophic lateral sclerosis, and the prion protein associated with Creutzfeldt-Jacob's disease (the "mad cow" disease in cattle) (reviewed in [5]).

The forming of the amyloid fibrils has certain similarities to a crystallization process, and may be considered an analogous phenomenon. At the beginning a nucleus is formed, which then grows and gives rise to soluble intermediates, which finally aggregate into insoluble fibrils. In the nomenclature used here, we will refer to the observable participants in the amyloid formation process as "monomers", "oligomers", and "protofibrils" (all soluble) together with "fibrils" (insoluble)—c.f. Ref. [6]. "Aggregates" is a more general term that will be used for both amyloid and non-amyloid forms of molecular assemblies. Whereas it was originally believed that the amyloid fibrils were the culprits causing neuronal damage in AD, the oligomeric states are now generally considered the most neurotoxic ones [1, 6], although maybe not the only toxic species. The amyloid cascade hypothesis formulated more than two decades ago [7, 8] is still valid, albeit with some modifications. A suggested mechanism of toxicity is membrane integrity disruption (e.g., transient pore formation) evoked by oligomeric and/or aggregating Aβ, causing ion dyshomeostasis and subsequent cell death [9, 10].

Amyloid material, understood in a broader sense, is on the borderline between being soluble and insoluble in aqueous solution. The monomers and the intermediate states along the fibrillation pathways leading to amyloid fibrils are water soluble and can often be visualized by various spectroscopic methods. Labeling of oligomeric amyloid intermediates or fibrillar states may be performed by small molecules such as Congo Red, which exhibits birefringence when bound to amyloid material, or Thioflavin T (ThT), which becomes strongly fluorescent upon binding [11, 12]. The specific binding of these dyes, or by specific antibodies, may be considered an alternative operational definition of amyloid, in vitro. Antibodies that specifically bind to oligomeric and fibrillar states have been developed [13]. The more detailed structural definitions of oligomeric and protofibrillar amyloid states are more elusive. A protofibril can be considered a short and soluble fibril with mostly β-structure, whereas an oligomeric state would appear earlier along the aggregation pathway and displays a loosely defined weak β-structure with no dominating fibril elongation. However, the detailed molecular and structural characteristics of a "toxic Aβ oligomer" still remain to be defined and determined [14].

Among structure determination methods, electron microscopy (EM) can be applied to the oligomeric, protofibrillar and fibrillar states but does not provide atomic-resolution data. X-ray crystallography is generally not possible with fibrillar material, since suitable crystals cannot be formed except from rather short peptides [15, 16]. Solid-state NMR (ssNMR) has proven a successful method for obtaining information on fibrillar structures with atomic resolution [17, 18], while solution NMR gives detailed information about molecular interactions and dynamics [19], mainly for the monomeric state. Indirect information about oligomeric states can however be obtained via advanced solution NMR techniques [20–22].

This minireview describes some recent NMR and EM results regarding the Aβ peptides. A special focus is placed on metal ion interactions with Aβ, as metal ions such as Cu(II) and Zn(II) are considered important for the outcome of the Aβ aggregation processes. The review is dedicated to the memory of Professor Ivano Bertini, who was a pioneer in the field of paramagnetic metal ion effects in NMR [23, 24], but who also recently contributed new ssNMR insights on Aβ fibril structures [25].

Structures of the monomeric Aβ peptide

Prior to proteolytic release from the membrane-bound APP, Aβ is mainly α-helical

The Aβ peptides are cleavage products created by proteolytic degradation of the membrane-associated APP [26]. Prior to proteolysis, the C-terminus of the Aβ region K28 to V40/A42 (Aβ numbering, Fig. 1a) is located in the hydrophobic membrane interior. To avoid free hydrogen bond partners, this region has to adopt a secondary structure or form supramolecular complexes. No high-resolution structure of the full-length APP is yet available, but the transmembrane region has been modeled to adopt an α-helical conformation. The central part of the Aβ peptides, i.e., Q15 to N27, resides in the interface between the apolar interior of the membrane and the polar head-group region. The N-terminus of the Aβ region in APP points out from the membrane and into the extracellular space [27]. A recent study by the Sanders group has shown that before cleavage of APP by γ-secretase inside the membrane, the transmembrane domain of APP is a flexibly curved α-helix [28]. Upon cleavage of APP, the Aβ peptides are released as mainly unstructured monomers. From the hydrophobicity of the primary structure Aβ can be divided into four
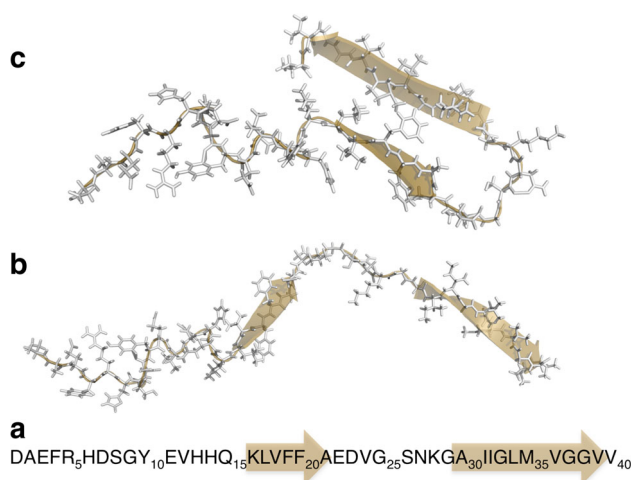
c

b

a

DAEFR₅HDSGY₁₀EVHHQ₁₅KLVFF₂₀AEDVG₂₅SNKGA₃₀IIGLM₃₅VGGVV₄₀

Fig. 1 The two hydrophobic regions L17–A21 and A30–V40 exhibit a secondary structure propensity for β-structure and are highlighted as arrows in the primary structure (**a**). These regions transiently adopt β-conformation (**b**) and may in turn transiently fold into a hairpin (**c**)

regions: two hydrophobic and two hydrophilic (Fig. 1a). The 16 first N-terminal residues constitute a hydrophilic tail. The two hydrophobic regions are the central L17–A21 part and the C-terminus A30–V40/A42, which are separated by the hydrophilic central region E22–G29.

Secondary structure propensity of monomeric Aβ in solution

Although the Aβ monomers are intrinsically disordered [29], they adopt mainly helical conformations when introduced to an apolar environment. When Aβ is added to the micellar form of the simple membrane-mimetic sodium dodecyl sulphate (SDS) or its lithium salt (LiDS), the hydrophobic regions fold into helices [30, 31]. Addition of paramagnetic Mn(II) to the Aβ–SDS mixture has revealed that the C-terminal helix is buried into the interior of the micelle, while the central helix is positioned on the surface of the micelle, only partially buried [31]. This may reflect the positioning of the Aβ region prior to cleavage from APP, and it underlines the ability for monomeric Aβ to adopt secondary structures.

In general, intrinsically disordered proteins (IDPs) and peptides possess, despite the lack of overall structure, transient structures or secondary structure propensities. Aβ monomers are no exception, as they display a number of properties indicating a secondary structure propensity [32, 33]. As a coarse-grained assessment of Aβ-structure, the overall apparent size of both full-length and truncated Aβ has been determined from the hydrodynamic radii, R_H, by PFG NMR. The relation between R_H and the monomer length, i.e., the scaling exponent v, was found to be substantially smaller (0.44) than what would be expected for a

corresponding excluded-volume statistical coil (0.58) [34]. This was interpreted as Aβ transiently forming more compact structures, either as global collapses or as secondary structure formations. Indeed, a more recent study showed that IDPs generally are more compact than denatured globular proteins, and an average v for IDPs was determined to be 0.45, in good agreement with findings for Aβ. This shows that Aβ may behave similarly to other IDPs that adopt transient structures [35].

The secondary structure of Aβ monomers has been studied by circular dichroism (CD) in numerous studies, and the CD spectrum of Aβ in room temperature shows all characteristics of a random coil spectrum. However, reducing the temperature induces gradual changes in the spectrum that correspond to an increased population of left-handed polyproline type 2 helix (PPII) [36, 37]. Similar structural changes have been found in other IDPs upon lowered temperature. PPII is an extended conformation, possibly facilitated by steric interactions between bulky side chains. The dihedral angles in PPII are very close to that of an aggregation-prone β-conformation. Although CD gives no information on a residual level, peptide truncation studies indicate that the Aβ PPII helix mainly involves the N-terminal region [37].

In addition, the hydrophobic regions appear to undergo temperature-induced structural changes. Determination of $^3J_{HNH\alpha}$ couplings indicates that the hydrophobic regions tend to have a β propensity in aqueous solution [37]. NMR relaxation measurements have shown that the transient secondary structures in these regions give rise to reduced motional freedom and restricted dynamics relative to the more flexible N-terminal region [38]. The Aβ regions that form helices in membrane-mimetic environments transiently form extended conformations rather than helical conformations in solution (Fig. 1b). The temperature dependence is typical for such transient structures: the extended PPII structural propensity shows a cooperative transition to random coil already at relatively low temperatures, i.e., the melting temperature is significantly lower than physiologically relevant temperatures [38].

Using detailed chemical shift analysis, Hou et al. [39] has showed that the propensity to form β conformations is reduced when M35 is oxidized, indicating transient long-range cross talk in monomeric Aβ.

Transiently folded states of Aβ

In NMR studies of Aβ not only chemical shifts, J-couplings, and relaxation parameters have been found to be temperature dependent, but a temperature increase also induces a general loss in ^{1}H-[^{15}N]-HSQC signal intensity. This was initially thought to be caused by increased exchange rates of the unprotected amide protons. However,

Yamaguchi et al. [40] found that also the intensities of $^1H\alpha$–$^{13}C\alpha$ correlations in ^1H-[^{13}C]-HSQC experiments were markedly decreased with increasing temperature. This signal intensity loss is most pronounced in the central hydrophilic D23–A30 region, and as it was attributed to chemical exchange line broadening, it suggested that the central region is involved in structural exchange. The authors suggested that Aβ monomers in solution adopt a transient hairpin-like conformation, where residues D23 to K30 are directly involved in the hairpin formation [40]. Earlier work by Lazo et al. [41] had already shown the central hydrophilic A21–A30 region of Aβ monomers to be protease resistant, indicating a folded non-random conformation. Indeed, NMR measurements and theoretical studies of this peptide segment alone have revealed the presence of a well-defined hairpin involving V24 to K28, and this has been proposed to be the 'folding nucleus' of Aβ [41, 42].

Transient structures of soluble monomeric Aβ affect aggregation and amyloid formation

The monomeric soluble Aβ transiently forms structures at various levels. The hydrophobic regions have a propensity for β-structure formation, and in the central hydrophilic region a turn can transiently be formed, bringing the two β-regions together. If these events occur simultaneously an overall transient fold of Aβ is produced, which may be modeled as in Fig. 1c. The resulting structure is similar to those found in the fibrils of aggregated Aβ. It is tempting to hypothesize that aggregation occurs by joining Aβ monomers in their transiently folded forms. This scenario is supported by Hou's finding that oxidation of M35, which reduces the β-structure propensity of Aβ monomers, also reduces aggregation and fibril formation [39]. Similar results have been obtained for other proteins, suggesting that β-structure propensity in certain peptide segments significantly enhances a protein's aggregation and amyloid formation capacity [43–45]. A similar case is the synucleins: Marsh et al. [46] found that the main difference between the amyloid-forming α-synuclein (αSN) and the much less aggregation-prone γ-synuclein (γSN) is the difference in secondary structure propensity. While αSN has a β-structure propensity in the amyloid-forming region, γSN has a propensity for helix formation. Tjernberg et al. [47] showed in a small peptide study that in addition to β-structure propensity, also charge attraction seems to be of importance for amyloid formation.

Hairpin structures of the Aβ peptide

Due to its transient nature, the proposed hairpin-like conformation of Aβ monomers has not been structurally determined. It is therefore of interest that an engineered binding protein, the so-called $Z_{A\beta3}$ affibody molecule, was found to bind monomeric Aβ in a hairpin conformation [48]. $Z_{A\beta3}$ was selected by phage display from a combinatorial protein library, and binds Aβ monomers with a K_d of 17 nM—thereby preventing its aggregation. A high-resolution NMR structure of the Aβ/$Z_{A\beta3}$ 1:2 complex shows that Aβ has adopted a hairpin structure, with residues 17–23 and 30–36 forming the hairpin legs and residues 24–29 forming the loop [48]. Intramolecular H-bonds are present both in the loop and between the two hairpin legs, although the legs and the loop also form intermolecular H-bonds with affibody residues. An intriguing possibility is whether the structure of Aβ observed in the Aβ/$Z_{A\beta3}$ complex is the same as the transient Aβ hairpin conformation when the affibody is absent. Binding to the affibody induces folding of Aβ, and folding upon binding is a normal event for unstructured proteins upon interaction with a specific binding partner. Disordered proteins tend to transiently adopt a structure resembling the bound state, and in this case this particular Aβ-conformation seems to be populated also in solution (c.f. Fig. 1c). One could imagine that the hairpin conformation is long-lived enough to allow formation of a series of intermolecular H-bonds with other Aβ hairpins, and as others have suggested, this might be how the Aβ aggregation process is initiated. On this note, it should be pointed out that certain enzymes that selectively degrade amyloidogenic peptides, such as the insulin-degrading enzyme (IDE) which acts on e.g., insulin and Aβ, target the peptide monomers in their β-sheet hairpin conformations [49].

The Aβ/$Z_{A\beta3}$ complex is also relevant insofar as the Aβ N-terminus is not part of the structured complex. Instead, the N-terminus sticks out and moves relatively freely, just like it does in the free Aβ monomer (whether unstructured or in a transient hairpin). Thus, the Aβ/$Z_{A\beta3}$ complex allows the monomeric Aβ N-terminus to be studied in an aggregation-free system. For example, as the Aβ N-terminus binds metal ions (see below), improved truncated non-fluorescent $Z_{A\beta3}$ versions have been developed that allow metal binding to the N-terminus of Aβ to be investigated without the usual metal-induced aggregation [50, 51].

Protein engineering has, furthermore, been employed to create an Aβ monomer locked in a hairpin conformation. Simultaneous A21C and A30C substitutions allowed formation of an intramolecular C21/C30 disulfide bridge holding the two hairpin legs in place (Fig. 2b) [52]. These modified Aβ peptides—named Aβ$_{CC}$—readily aggregate into oligomers and protofibrils along various pathways, but never form mature fibrils. One hypothetic model for fibril formation requires that the hairpin legs are rotated so that the intramolecular H-bonds can be transformed into
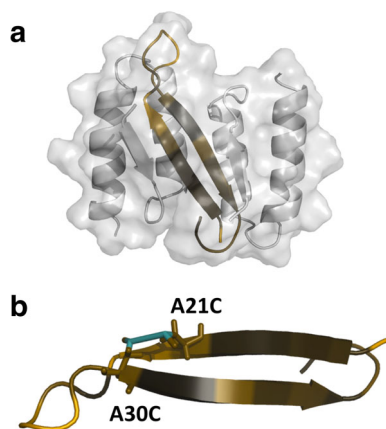
Fig. 2 β-Hairpin conformation stabilized in monomeric Aβ(1–40) in complex with the affibody protein $Z_{Aβ3}$ (**a**) and by an intramolecular disulfide bond in a double cysteine mutant (**b**). Hydrophobicity is indicated as color scheme from brown (hydrophobic) to orange (hydrophilic). Structures were created after the pdb structure 2OTK and the works of Hoyer et al. [48] and Sandberg et al. [52] for **a** and **b**, respectively

intermolecular H-bonds, thus creating the possibility to form parallel and in-register β-sheets. This particular $Aβ_{CC}$ S–S bridge obviously hinders the formation of the cross-β-sheet entity. If the $Aβ_{CC}$ S–S bridge is removed via a reducing agent, however, proper fibrils are formed. $Aβ(1–40)_{CC}$ and $Aβ(1–42)_{CC}$ aggregated along different pathways and yielded aggregation products with different toxicity. The $Aβ(1–42)_{CC}$ oligomers and protofibrils were highly neurotoxic, indicating that hairpin conformation is one, but not the only, important factor for Aβ toxicity [52]. Understanding the nature of the differences in toxicity and aggregation pathways between $Aβ(1–40)_{CC}$ and $Aβ(1–42)_{CC}$ may help explain why certain Aβ mutations lead to early onset AD.

Metal ion interactions with the Aβ peptide

Several lines of evidence have shown that both soluble and aggregated forms of Aβ bind and coordinate divalent metal ions, such as Cu(II) and Zn(II). Metal binding may be accompanied by a disturbance in metal homeostasis (or conversely), and the AD brain is indeed characterized by metal dyshomeostasis [53, 54]. Metal ions have been proposed to be, directly or indirectly, involved in the neurodegenerative mechanisms of AD [54]. In the Aβ aggregation end-states, i.e., the amyloid plaques, there is colocalization of metal ions such as Zn, Cu, and Fe ions, and the Aβ peptide coordinates the metals with relatively high affinity [55]. The various aspects of Aβ/metal ion interaction have been studied with a wide range of techniques, e.g., NMR, EPR, fluorescence, and theoretical approaches [19].

Quantitative aspects

When discussing the dissociation constant, K_d, that describes binding of a metal ion to the peptide molecule, it is imperative not to compare K_d values obtained under different conditions. Several buffers often used in in vitro studies of Aβ–metal interactions coordinate metals and bias the affinity estimation. In the case of Cu(II) it is possible to calculate the buffer-independent apparent K_d. This however requires that all Cu(II)-binding components in the solution are taken into account. Furthermore, aggregated forms of Aβ appear to have an affinity for metal ions that is several orders of magnitude higher compared to soluble monomers, implying that also very minute amounts of aggregates, likely to be found in any sample, will affect the binding measurements. Further complications arise from the metal ions affecting both oligomer and aggregation formation, thereby causing the metal-binding affinity of the system to change over time in a condition-dependent manner that includes both peptide and metal concentration. No real consensus has been reached for the Cu(II) affinity of monomeric Aβ, and differences in reported dissociation constants may arise from (1) the formation of metal–buffer ternary complexes that are left unaccounted for [56]; (2) the different structural states of the peptide (both the various lengths of peptide that have been used as well as the aggregation state of the peptide) [57]; (3) the ambiguity of the stoichiometry of the complex [58]; and (4) the possibility of systematic and model errors in the method for affinity determination. Despite the ongoing debate, the apparent K_d value for Aβ-fibrils, aggregates and monomers should fall in the wide range of 10^{-11}–10^{-6} M [58–63].

The reported Aβ/Zn(II) affinities are slightly lower than the Aβ/Cu(II) affinities, and the buffer-uncorrected apparent dissociation constants fall in the range of 1–60 μM [57, 63]. However, competition experiments indicate that the Aβ affinity for Zn(II) is comparable to that for Cu(II), under similar conditions [63]. Again, some of the observed variability in the Aβ/Zn(II) binding constant arguably derives from different Aβ forms being present during the experiment, as Aβ affinity for Zn(II) has been shown to rise during aggregation [59].

Although copper affinity to soluble monomeric Aβ is several orders of magnitude lower than the affinities to copper chaperone systems [64, 65], aggregated Aβ has been shown to harbor copper in vivo. This indicates that in vivo, the affinity of Aβ aggregates for copper falls into the biologically relevant range. For monomeric Aβ, the Cu(II) and Zn(II) affinities may be physiologically relevant in case of local or global metal dyshomeostasis.

Binding of Aβ to metal ions may induce a variety of in vitro and in vivo effects. The metal ions can influence peptide aggregation and fibrillation, both regarding kinetics

and aggregation pathways [66]. Interestingly, the effect on Aβ aggregation is dose-dependent, i.e., low sub-stoichiometric concentrations of divalent metals are suggested to reduce oligomeric stability and protect from aggregation [67], while higher metal concentrations produce amorphous aggregation [68]. Such formation of amorphous aggregates may protect from oligomer and amyloid formation. However, these amorphous aggregates are not dead-end products of the aggregation pathway. It has been demonstrated that they may evolve into fibrils [69] or spherical aggregates [70]. Inhibition of amyloid fibril formation can be monitored by ThT fluorescence kinetics experiments, and Yoshiike et al. [71] has demonstrated that Zn(II) and Cu(II) prevent the formation of ThT-active fibrillar structures at a stoichiometric ratio of 1:2 Aβ:metal ion. Instead, the amount of amorphous aggregates increases, as revealed by significant signal losses in CD experiments on metal-induced Aβ aggregates [72].

In addition to the aggregation propensity effects, binding of redox-active Cu(II) to Aβ may prompt the formation of reactive oxygen species, which in turn may cause oxidative damage to neurons [73]. Such damage may be involved in AD pathology, which is why Cu(II) has been suggested as a possible causative agent behind AD. On the other hand, chelation of Zn(II) by amyloid aggregates may induce cognitive loss due to local depletion of extracellular Zn [53]. In fact, in vitro cell toxicity studies of metal depleted SOD1 have shown that local zinc chelation by apoSOD1 is an effective neurotoxic mechanism, and that this toxicity can be abolished by zinc addition. In line with this observation, addition of zinc to a cell culture also reduces the Aβ toxicity [74, 75].

Structural aspects of metal binding

Despite the consensus regarding the importance of Aβ–metal interactions, no high-resolution structure of low molecular weight Aβ in complex with metal ions is available, and the ligands involved are still debated. The reason for this lack of structural information might be that the metal ions do not induce a specific structure, but rather an ensemble of structures. The conformation and coordination of the peptide–metal ion complex seem to depend on the experimental conditions. However, the minimal metal-binding site of the Aβ peptide has been identified to consist of the first 16 N-terminal amino acids [76], and the structure of a 16-mer peptide model in complex with zinc has been solved by NMR [77]. The four metal ligands were found to consist of the side chains of H6, E11, H13, and H14 (Fig. 3a). In contrast to this structure, several other metal-binding modes for the N-terminal peptide Aβ(1–16) have been suggested from EPR/NMR experiments, and the Aβ(1–16)/Cu(II) complex can adopt at least two additional

different structures, depending on the pH [78]. In this truncated variant and in longer truncated peptides, i.e., Aβ(1–28), the ligands involved in metal binding have been suggested to be the histidines and/or D1 [79], A2 [78], E3 [80], R5 [81], or E11 [79]. This variety of proposed ligands underlines the difficulties in determining a single structural state of the complex, and arguably reflect the diversity of metal-binding conformations in the truncated Aβ variants, and possibly also in the native peptide.

For the full-length peptide, a number of biophysical studies show that the three His residues are involved in metal coordination. The N-terminus [63, 82, 83], D1 [84], Y10 [85], or coordinated H_2O [86] are the proposed candidates for the fourth ligand. However, in NMR experiments on Aβ(1–40) at physiological pH, R5, Y10 and E11 showed no chemical shift changes or line broadening upon addition of metal ions, indicating that they are not involved in metal ligation [63]. The cross peak of D1 in a ^1H-[^{13}C]-HSQC spectrum on the other hand, is shifted and line broadened when zinc is added. This indicates that D1 is involved in Zn binding, either through the N-terminus or the D1 side chain (c.f. structural models in Fig. 3b, c). Several studies have suggested that metals may serve as bridges between Aβ molecules, thereby forming higher-order complexes, which may serve as a mechanistic explanation for metal-induced amorphous aggregation [87].

Recent NMR studies of zinc binding to Aβ(1–40) suggest that N-terminal metal binding induces a turn in the central hydrophilic region, indicating long-range cross talk in the peptide and again highlight the propensity for turn-formation in full-length Aβ [83].

The apparent contradictions between the metal-binding results for Aβ(1–16/28) and Aβ(1–40) may reflect an involvement of the C-terminus in the overall full-length Aβ/Zn(II) structure. In fact, the C-terminus has been proposed to be involved in metal coordination in the aggregated state of Aβ, c.f. next chapter.

Solid-state NMR studies of Aβ fibril structures

Solid-state NMR (ssNMR) has made major contributions to our understanding of the molecular structures of amyloid fibrils. Different aspects of amyloid fibril structures, studied by ssNMR, have been covered in recent review articles [18, 88].

Aβ(1–40) fibrils are typically straight and unbranched, have diameters on the order of 10 nm, and contain ribbon-like β-sheets where the β-strands run approximately perpendicular to the long fibril axis, while the inter-strand hydrogen bonds run approximately parallel to the long fibril axis. Amyloid fibrils are intrinsically insoluble and
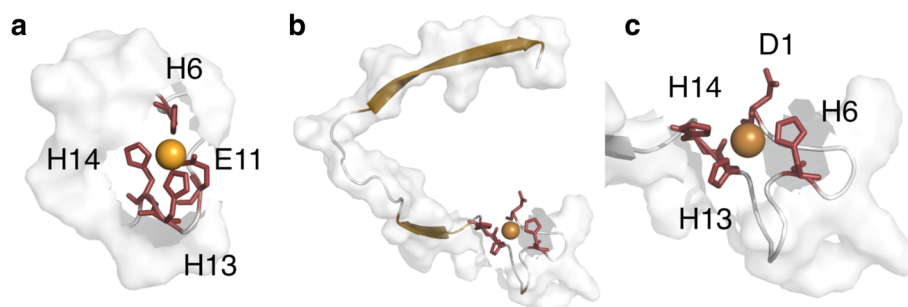
Fig. 3 The metal-binding site for Aβ(1–16), constructed using PDB ID 1ZE9 consists of the ligands H6, H13, H14 and E11 (**a**) while for Aβ(1–40) the fourth ligand is assigned to D1 (**c**). The full-length peptide, including the metal-binding site and its regions with β-structure propensity, is depicted in **b**. Structures in **b** and **c** are modeled from NMR data in [63]

Fig. 4 Two stacked protofilaments with cross-β structure of Aβ(1–40) (**a**) and the cross-β structure of Aβ(1–42) of a single protofilament (**b**) were created after the pdb structures 2LMN (Ref. [114]) and 2BEG (Ref. [95]) for **a** and **b**, respectively
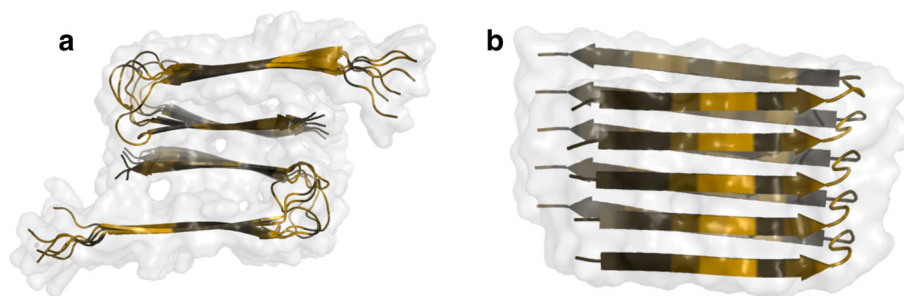
non-crystalline, and are therefore not amenable to high-resolution structure determination techniques such as X-ray crystallography or high-resolution solution NMR spectroscopy. ssNMR techniques have been particularly valuable as ssNMR measurements on isotope-labeled samples have the unique capability of providing detailed structural constraints in non-crystalline, fibrillar structures. With complementary long-range constraints obtained from EM or small-angle neutron scattering studies, and in combination with site-directed mutagenesis, it has proven possible to develop full structural models for amyloid fibrils from solid-state NMR data. Such models reveal both the molecular conformation and the supramolecular organization (Fig. 4).

Intrinsic sample polymorphism of Aβ fibrillar structures is a major obstacle for ssNMR studies, as it results in samples with low structural homogeneity. Nevertheless, a consensus structure for Aβ peptides has been obtained, describing a β-hairpin with a turn in the 25–29 region. ssNMR data show that the cross-β motifs in Aβ(1–40) fibrils are comprised of parallel β-sheets, while those in Aβ(11–25) fibrils are comprised of antiparallel β-sheets. Studies with ssNMR on amyloid fibrils prepared in vitro from synthetic Aβ peptides have shown that the molecular structure of Aβ(1–40) fibrils is not uniquely determined by the amino acid sequence. Instead, the fibril structure also depends on the precise details of the growth conditions [89]. The earliest ssNMR studies on Aβ peptides were

performed by Lansbury et al. [90–92] on the nine amino acid Aβ(34–42) peptide. Multiple-quantum ssNMR measurements indicate a parallel organization of β-sheets in Aβ fibrils [93]. NMR dipolar recoupling methods for the measurement of inter-peptide distances have established that the central core of Aβ(10–35) consists of a parallel β-sheet structure where identical residues in adjacent chains are in register [94]. The 3D structure of an Aβ(1–42) protofilament shows two stacked, intermolecular, parallel, in-register β-sheets that perpetuate along the fibril axis [95]. This structure has been used as a docking model in theoretical calculations to facilitate development of new Aβ fibrillation inhibitors [96].

Studies on the Aβ Iowa mutant (D23N), which is associated with early onset neurodegeneration, indicate that Aβ(1–40) Iowa-mutant fibrils formed in vitro can contain either parallel or antiparallel β-sheets [97]. Experiments in neuronal cell cultures demonstrated that both forms were cytotoxic.

A recent ssNMR structure of the wild type Aβ(1–40) interprotofilament interface reported by Ivano Bertini's group [25] differs from previously published structures, again showing how the fibril structures depend on the preparation methods and conditions. Somewhat surprisingly, the high quality of the NMR spectra obtained by Bertini's group indicates a high molecular homogeneity of the fibrils. Nevertheless, an emerging consensus picture supports the polymorphism of fibril structure morphology,

possibly with multiple structures co-existing, even though all tertiary structures are based on parallel in-register β-sheet secondary structures, generally showing hairpin variants. The fibril cross-sections display either twofold or threefold symmetry regarding the arrangement of the ordered hairpins.

A very recent study by the Tycko group [98] shows the molecular structure of a Aβ(1–40) fibril grown from a seed of a human brain extract. ssNMR spectra recorded for fibrils seeded from two AD patients were significantly different. From one of the seeded fibrils it was possible to determine a detailed and unique structure. The fibril cross-section showed a threefold symmetry unit based on three hairpin structures. The observation that the seeded fibrils contained two clearly different Aβ conformations makes the Aβ fibrillation process reminiscent of the propagation of different prion strains [99]. Indeed, it has been proposed that also Aβ assemblies are capable of self-propagation inside the human brain [100].

Bertini's group has also developed a method known as sedimented solutes NMR (SedNMR), in which ssNMR experiments are used to observe proteins that are sedimented from solution via an ultracentrifugal field [101].

ssNMR studies on Aβ fibrils have also been used to investigate binding sites and binding structures of Cu(II) to Aβ [102]. The molecular details of Cu(II) binding to amyloid Aβ(1–40) fibrils were probed using paramagnetic signal quenching in 1D and 2D high-resolution ^{13}C ssNMR. Selective quenching observed in ^{13}C spectra of Cu(II)-bound Aβ(1–40) suggested that primary Cu(II) binding sites in Aβ(1–40) fibrils include N^{ε} in H13 and H14, together with carboxyl groups in V40 as well as in glutamic acid side chains (i.e., E3, E11, and/or E22). ^{13}C chemical shift analysis demonstrated no major structural changes upon Cu(II) binding in the hydrophobic core regions (residues 18–25 and 30–36) of Aβ. Although, the occurrence of ROS production via oxidization of M35 in the presence of Cu(II) has long been suspected, the $^{13}C^{\varepsilon}H_3$-S signal in M35 showed little change after Cu(II) binding, demonstrating that M35 cannot be oxidized by Cu(II) alone.

In summary, ssNMR spectroscopy is a powerful technique for structural studies in amyloid fibrils that deepened our understanding of the structure of the fibril and the process of its formation.

Cryo-electron microscopy studies of Aβ fibrils

Biological structures can be visualized in the electron microscope (EM), but the combined effect of poor contrast and radiation damage makes it difficult to achieve high-resolution images. Negative staining with salts of heavy atoms followed by dehydration can enhance contrast. However, this compromises resolution, as the staining procedure induces random structural distortions at the molecular level. Alternatively, the sample can be maintained in a hydrated state and—to a limited degree—be protected against radiation damage by rapid freezing and imaging at liquid N_2 temperatures. This technique preserves resolution, but suffers from poor contrast. By combining advanced microscopes, the latest electron detectors, and dedicated image processing algorithms, contrast can be enhanced by averaging 2D images of many identical molecular structures into a 3D structure. This approach is especially attractive for structures with internal symmetry: icosahedral viruses have been visualized to almost 3 Å resolution [103], and 3D images of protein nanocrystals suggest that atomic resolution might be around the corner [104]. The 1D crystalline nature of the Aβ peptide helical fibrils makes them an attractive target for cryo-EM. Cross-sections of fibrils (Fig. 5a, b) as well as details of fibril structures (Fig. 5c) may be determined. Platinum shadowing (not a cryo-EM technique) has shown that Aβ(1–40) fibrils exhibit periodic cross-β structures with a left-handed supertwist. In a 3D cryo-EM reconstruction (2.6 nm resolution), these fibrils were shown to have a ribbon-like shape and had a clear polarity [105]. Extension of the resolution to 8 Å revealed that the fibril consists of two protofilaments, each containing ∼5 nm long regions of β-sheet structure (Fig. 5b). Cross-sections showed two Aβ(1–40) peptides folded symmetrically into a paired β-sheet structure [106]. This is in agreement with the super structure formed by a smaller Aβ peptide, solved by X-ray crystallography [16]. The fibrils are homogeneous in width, but significantly vary in their helical pitch. Two subgroups of Aβ(1–40) fibrils were distinguished: F120 and F140 fibrils, with a helical repeat (cross-over distance) of (120 ± 10) nm and (140 ± 10) nm, respectively [107]. In cross-section, F120 and F140 are highly similar and their difference may be arbitrary [107].

The Aβ(1–42) fibrils are markedly different from cryo-EM models of Aβ(1–40) fibrils. Proteolysis analysis and iterative real-space helical reconstruction has revealed that two protofilaments form an interprotofilament with a hollow core that holds the Aβ(1–42) C-terminus (Fig. 5a) [108]. Thus, the large hydrophobic C-terminal residues are buried inside the fibril, something that presumably also increases fibril stability (Fig. 5d). In cross-section, the protofilament measures around 40 Å × 20 Å [108], a density into which the ssNMR hairpin structure of the peptide [95] could be fitted. It has been proposed that the flexible N-terminus of Aβ(1–42) might stack on the hairpin loop of another Aβ(1–42) unit [108]. Even within a single preparation morphological diversity of Aβ(1–42) fibrils was observed, which may have several causes. For
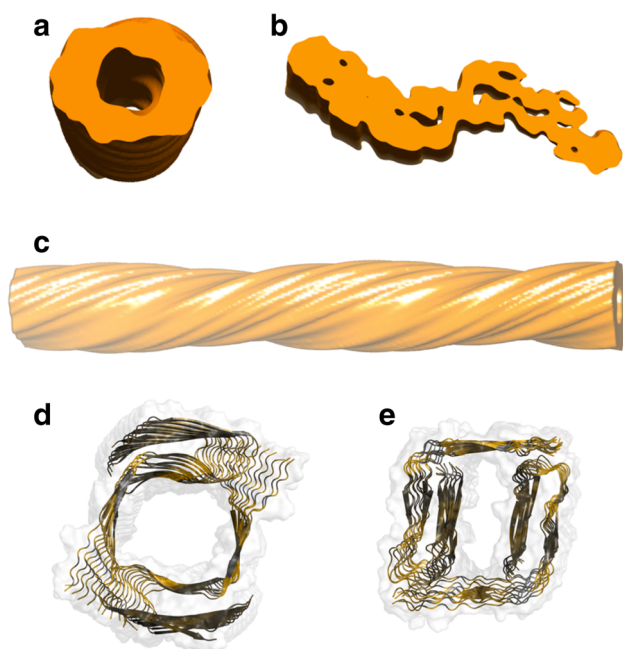
Fig. 5 Cross-section of **a** Aβ(1–42) fibril images (accession no EMD-5052; Ref. [108]) and **b** Aβ(1–40) fibril images (accession no EMD-5008; Ref. [106]) obtained via cryo-EM studies. The fibrils were modeled and sliced using the *ucsf chimera* visualization system [115]. **d**, **e** Two possible models for Aβ(1–42) fibrils, created by fitting in two ways an existing ssNMR structure of Aβ(1–42) (Ref. [109]) into fibril conformation **c**, which was mapped using cryo-EM

example, the weak interaction between the N-terminus of one peptide with the C-terminal hairpin of another may result in several different potential conformations, which each could induce a different organization of the fibril assemblies in the different protofilament regions. Alternatively, the flexibility of the unstructured Aβ(1–42) N-terminus could play an important role in the packing/stability of protofilament assemblies. Using the Aβ(1–42) fibril density map from cryo-EM and the hairpin structure of Aβ(1–42) from ssNMR, Miller et al. [109] employed molecular dynamics to study the stability of the hollow core protofilament structure at different pH values. The modeled pH-dependent differences in peptide packing in the protofilament assemblies may explain the structural heterogeneity of the pH variants (Fig. 5d, e). The most stable fibril structure was that with the C-termini facing the external surface (Fig. 5d) [109].

A comparison between the models of Aβ(1–40) and Aβ(1–42) fibrils shows that both have different characteristics, but also share many structural features. Both Aβ(1–40) and Aβ(1–42) mature fibrils consist of pairs of protofilaments that twist around each other. The protofilaments of Aβ(1–40) and Aβ(1–42) display similar structures with twofold axial symmetry [110]. However, Aβ(1–42) protofilaments have a hollow core, whereas there is ordered

density around the central axis of the Aβ(1–40) fibril. The cross-section maps of Aβ(1–40) and Aβ(1–42) fibrils indicate that the interactions between the protofilaments are controlled by the flexible, unstructured N-termini of the peptides. Aβ(1–42) and Aβ(1–40) fibrils have different helical twists with cross-over distances of 200–400 and ∼1,425 Å, respectively. In addition, the diameter of Aβ(1–42) fibrils varies from 67 to 85 Å, whereas the diameter of Aβ(1–40) fibrils ranges from 60 to 200 Å [108].

The unstructured flexible Aβ N-terminus, which appears to regulate the assembly of Aβ protofilaments, might be developed as a drug target. The mechanism of Aβ fibrillation likely involves several steps: (1) Aβ peptide segments initially associate with each other; (2) then these small complexes pack into a protofilament, forming the β-sheet interface; (3) the protofilaments assemble to form a fibril, the morphology of which is modulated by the intermolecular interaction between the N- and C-termini. The helical reconstruction models from cryo-EM data have significantly enhanced our understanding of the mechanism of Aβ fibrillation and may explain why specific conformers are associated with neurodegenerative pathologies.

Final remarks

NMR spectroscopy, often together with EM microscopy, provides an abundance of information for a biophysicist trying to understand the structural properties of amyloid material and its formation in vitro, as a model for the in vivo processes associated with a variety of neurodegenerative diseases. Here, we have focused on the Aβ peptides associated with AD.

In modern NMR studies, isotopic labeling with ^{15}N and/or ^{13}C is usually required for detailed and selective results. Then, in the solid state, ssNMR together with molecular modeling can provide atomic-resolution information on the fibrillar structures formed by Aβ peptides. In solution state, the NMR signals are normally lost for the aggregated material, although particular methods such as relaxation dispersion [20, 22] or saturation transfer [21] can extract information on the structures and kinetics associated with the amyloid material in its "dark state" of NMR [21, 111]. Relatively simple solution experiments such as ^{1}H-[^{15}N]-HSQC can give the first clues about the interactions between monomeric Aβ and small molecules or metal ions, which often influence both the Aβ NMR spectra and the Aβ aggregation pathways (kinetically or structurally).

One structural feature standing out from a large number of recent in vitro studies is the Aβ hairpin, which appears as a building block in oligomeric and fibrillar higher-ordered structures. The details of the hairpin conformation may vary,

depending on the exact nature of the peptide sample and its environmental conditions, but the overall properties seem to converge. This more or less ordered hairpin, accompanied by a less-structured N-terminus, is probably the most important Aβ form that interacts with the environment and determines the continued process of aggregation. The observation that a fibril seeded from a human brain extract also shows this basic structural unit indicates that it is probably also relevant for human disease.

There are still many unresolved questions regarding the Aβ aggregation and fibrillation processes. Major questions concern the connection between the observations of the aggregation process in vitro and the disease aspects in vivo. Some examples of unresolved topics are:

- the structure(s) of the neurotoxic Aβ assemblies and what mechanism(s) causes neurotoxicity,
- the spreading of the neurotoxic assemblies between neurons and the potential similarities to prion disease mechanisms [98, 100, 112],
- the roles of metal ions, redox active and inactive, in the neurotoxic processes involving the Aβ peptide [113], and
- the possibility to base drug development on the in vitro observations of the Aβ peptide aggregation process.

The gap of knowledge between in vitro studies and understanding of in vivo pathology in humans is at present visible in the disturbing lack of reliable and relevant model systems as well as absence of structure–toxicity relationship, as the in vitro observations alone may not be sufficient to develop a detailed mechanistic understanding of the in vivo disease manifestations.

Despite the encouraging progress made in molecular amyloid research during the last decade, much more knowledge is needed before we can formulate therapeutic strategies for the associated devastating diseases.

References

1. Haass C, Selkoe DJ (2007) Nat Rev Mol Cell Biol 8:101–112
2. Masters CL, Selkoe DJ (2012) Cold Spring Harb Perspect Med 2:a006262
3. Sunde M, Blake CC (1998) Q Rev Biophys 31:1–39
4. Eisenberg D, Jucker M (2012) Cell 148:1188–1203
5. Chiti F, Dobson CM (2006) Annu Rev Biochem 75:333–366
6. Fändrich M (2012) J Mol Biol 421:427–440
7. Selkoe DJ (1991) Neuron 6:487–498
8. Hardy JA, Higgins GA (1992) Science 256:184–185
9. Butterfield SM, Lashuel HA (2010) Angew Chem Int Ed Engl 49:5628–5654
10. Lashuel HA, Hartley D, Petre BM, Walz T, Lansbury PT Jr (2002) Nature 418:291
11. Biancalana M, Koide S (2010) Biochim Biophys Acta 1804:1405–1412
12. Skeby KK, Sørensen J, Schiøtt B (2013) J Am Chem Soc 135:15114–15128
13. Necula M, Kayed R, Milton S, Glabe CG (2007) J Biol Chem 282:10311–10324
14. Benilova I, Karran E, De Strooper B (2012) Nat Neurosci 15:349–357
15. Nelson R, Sawaya MR, Balbirnie M, Madsen AØ, Riekel C, Grothe R, Eisenberg D (2005) Nature 435:773–778
16. Sawaya MR, Sambashivan S, Nelson R, Ivanova MI, Sievers SA, Apostol MI, Thompson MJ, Balbirnie M, Wiltzius JJ, McFarlane HT, Madsen AØ, Riekel C, Eisenberg D (2007) Nature 447:453–457
17. Fitzpatrick AW, Debelouchina GT, Bayro MJ, Clare DK, Caporini MA, Bajaj VS, Jaroniec CP, Wang L, Ladizhansky V, Muller SA, MacPhee CE, Waudby CA, Mott HR, De Simone A, Knowles TP, Saibil HR, Vendruscolo M, Orlova EV, Griffin RG, Dobson CM (2013) Proc Natl Acad Sci USA 110:5468–5473
18. Tycko R (2011) Annu Rev Phys Chem 62:279–299
19. Wärmländer S, Tiiman A, Abelein A, Luo J, Jarvet J, Söderberg KL, Danielsson J, Gräslund A (2013) ChemBioChem 14:1692–1704
20. Abelein A, Lang L, Lendel C, Gräslund A, Danielsson J (2012) FEBS Lett 586:3991–3995
21. Fawzi NL, Ying J, Torchia DA, Clore GM (2010) J Am Chem Soc 132:9948–9951
22. Abelein A, Kaspersen JD, Nielsen SB, Jensen GV, Christiansen G, Pedersen JS, Danielsson J, Otzen DE, Gräslund A (2013) J Biol Chem 288:23518–23528
23. Bertini I, Luchinat C, Parigi G, Pierattelli R (2005) ChemBioChem 6:1536–1549
24. Bertini I, Luchinat C, Parigi G, Pierattelli R (2008) Dalton Trans, 3782–3790
25. Bertini I, Gonnelli L, Luchinat C, Mao J, Nesi A (2011) J Am Chem Soc 133:16013–16022
26. De Strooper B, Saftig P, Craessaerts K, Vanderstichele H, Guhde G, Annaert W, Von Figura K, Van Leuven F (1998) Nature 391:387–390
27. Gralle M, Ferreira ST (2007) Prog Neurobiol 82:11–32
28. Barrett PJ, Song Y, Van Horn WD, Hustedt EJ, Schafer JM, Hadziselimovic A, Beel AJ, Sanders CR (2012) Science 336:1168–1171
29. Riek R, Guntert P, Dobeli H, Wipf B, Wüthrich K (2001) Eur J Biochem 268:5930–5936
30. Shao H, Jao S, Ma K, Zagorski MG (1999) J Mol Biol 285:755–773
31. Jarvet J, Danielsson J, Damberg P, Oleszczuk M, Gräslund A (2007) J Biomol NMR 39:63–72
32. Dyson HJ, Wright PE (2005) Nat Rev Mol Cell Biol 6:197–208
33. Lacy ER, Filippov I, Lewis WS, Otieno S, Xiao L, Weiss S, Hengst L, Kriwacki RW (2004) Nat Struct Mol Biol 11:358–364
34. Danielsson J, Jarvet J, Damberg P, Gräslund A (2002) Magn Reson Chem 40:S89–S97
35. Bernado P, Blackledge M (2009) Biophys J 97:2839–2845
36. Jarvet J, Damberg P, Danielsson J, Johansson I, Eriksson LE, Gräslund A (2003) FEBS Lett 555:371–374
37. Danielsson J, Jarvet J, Damberg P, Gräslund A (2005) FEBS J 272:3938–3949
38. Danielsson J, Andersson A, Jarvet J, Gräslund A (2006) Magn Reson Chem 44 Spec No:S114–S121

39. Hou L, Shao H, Zhang Y, Li H, Menon NK, Neuhaus EB, Brewer JM, Byeon IJ, Ray DG, Vitek MP, Iwashita T, Makula RA, Przybyla AB, Zagorski MG (2004) J Am Chem Soc 126:1992–2005

40. Yamaguchi T, Matsuzaki K, Hoshino M (2011) FEBS Lett 585:1097–1102

41. Lazo ND, Grant MA, Condron MC, Rigby AC, Teplow DB (2005) Protein Sci 14:1581–1596

42. Roychaudhuri R, Yang M, Condron MM, Teplow DB (2012) Biochemistry 51:3957–3959

43. Moriarty DF, Raleigh DP (1999) Biochemistry 38:1811–1818

44. Chiti F, Taddei N, Baroni F, Capanni C, Stefani M, Ramponi G, Dobson CM (2002) Nat Struct Biol 9:137–143

45. Simmons LK, May PC, Tomaselli KJ, Rydel RE, Fuson KS, Brigham EF, Wright S, Lieberburg I, Becker GW, Brems DN et al (1994) Mol Pharmacol 45:373–379

46. Marsh JA, Singh VK, Jia Z, Forman-Kay JD (2006) Protein Sci 15:2795–2804

47. Tjernberg L, Hosia W, Bark N, Thyberg J, Johansson J (2002) J Biol Chem 277:43243–43246

48. Hoyer W, Grönwall C, Jonsson A, Ståhl S, Härd T (2008) Proc Natl Acad Sci USA 105:5099–5104

49. Shen Y, Joachimiak A, Rosner MR, Tang WJ (2006) Nature 443:870–874

50. Lindgren J, Wahlström A, Danielsson J, Markova N, Ekblad C, Gräslund A, Abrahmsén L, Eriksson Karlström A, Wärmländer SKTS (2010) Protein Sci 19:2319–2329

51. Lindgren J, Segerfeldt P, Sholts SB, Gräslund A, Karlström AE, Wärmländer SK (2013) J Inorg Biochem 120:18–23

52. Sandberg A, Luheshi LM, Söllvander S, Pereira de Barros T, Macao B, Knowles TP, Biverstål H, Lendel C, Ekholm-Petterson F, Dubnovitsky A, Lannfelt L, Dobson CM, Härd T (2010) Proc Natl Acad Sci USA 107:15595–15600

53. Adlard PA, Bush AI (2006) J Alzheimers Dis 10:145–163

54. Ayton S, Lei P, Bush AI (2013) Free Radic Biol Med 62:76–89

55. Lovell MA, Robertson JD, Teesdale WJ, Campbell JL, Markesbery WR (1998) J Neurol Sci 158:47–52

56. Tõugu V, Tiiman A, Palumaa P (2011) Metallomics 3:250–261

57. Tiiman A, Palumaa P, Tõugu V (2013) Neurochem Int 62:367–378

58. Alies B, Renaglia E, Rozga M, Bal W, Faller P, Hureau C (2013) Anal Chem 85:1501–1508

59. Tõugu V, Karafin A, Palumaa P (2008) J Neurochem 104:1249–1259

60. Sacco C, Skowronsky RA, Gade S, Kenney JM, Spuches AM (2012) J Biol Inorg Chem 17:531–541

61. Rozga M, Kloniecki M, Dadlez M, Bal W (2010) Chem Res Toxicol 23:336–340

62. Sarell CJ, Syme CD, Rigby SE, Viles JH (2009) Biochemistry 48:4388–4402

63. Danielsson J, Pierattelli R, Banci L, Gräslund A (2007) FEBS J 274:46–59

64. Badarau A, Dennison C (2011) J Am Chem Soc 133:2983–2988

65. Jeney V, Itoh S, Wendt M, Gradek Q, Ushio-Fukai M, Harrison DG, Fukai T (2005) Circ Res 96:723–729

66. Suzuki K, Miura T, Takeuchi H (2001) Biochem Biophys Res Commun 285:991–996

67. Garai K, Sengupta P, Sahoo B, Maiti S (2006) Biochem Biophys Res Commun 345:210–215

68. Garai K, Sahoo B, Kaushalya SK, Desai R, Maiti S (2007) Biochemistry 46:10655–10663

69. Tõugu V, Karafin A, Zovo K, Chung RS, Howells C, West AK, Palumaa P (2009) J Neurochem 110:1784–1795

70. Pedersen JT, Ostergaard J, Rozlosnik N, Gammelgaard B, Heegaard NH (2011) J Biol Chem 286:26952–26963

71. Yoshiike Y, Tanemura K, Murayama O, Akagi T, Murayama M, Sato S, Sun X, Tanaka N, Takashima A (2001) J Biol Chem 276:32293–32299

72. Ghalebani L, Wahlström A, Danielsson J, Wärmländer SK, Gräslund A (2012) Biochem Biophys Res Commun 421:554–560

73. Huang X, Atwood CS, Hartshorn MA, Multhaup G, Goldstein LE, Scarpa RC, Cuajungco MP, Gray DN, Lim J, Moir RD, Tanzi RE, Bush AI (1999) Biochemistry 38:7609–7616

74. Cardoso SM, Rego AC, Pereira C, Oliveira CR (2005) Neurotox Res 7:273–281

75. Johansson AS, Vestling M, Zetterström P, Lang L, Leinartaite L, Karlström M, Danielsson J, Marklund SL, Oliveberg M (2012) PLoS ONE 7:e36104

76. Minicozzi V, Stellato F, Comai M, Dalla Serra M, Potrich C, Meyer-Klaucke W, Morante S (2008) J Biol Chem 283:10784–10792

77. Zirah S, Kozin SA, Mazur AK, Blond A, Cheminant M, Segalas-Milazzo I, Debey P, Rebuffat S (2006) J Biol Chem 281:2151–2161

78. Drew SC, Noble CJ, Masters CL, Hanson GR, Barnham KJ (2009) J Am Chem Soc 131:1195–1207

79. Gaggelli E, Janicka-Klos A, Jankowska E, Kozlowski H, Migliorini C, Molteni E, Valensin D, Valensin G, Wieczerzak E (2008) J Phys Chem B 112:100–109

80. Hureau C, Coppel Y, Dorlet P, Solari PL, Sayen S, Guillon E, Sabater L, Faller P (2009) Angew Chem 48:9522–9525

81. Zirah S, Rebuffat S, Kozin SA, Debey P, Fournier F, Lesage D, Tabet JC (2003) Int J Mass Spectrom 228:999–1016

82. Valiente-Gabioud AA, Torres-Monserrat V, Molina-Rubino L, Binolfi A, Griesinger C, Fernandez CO (2012) J Inorg Biochem 117:334–341

83. Rezaei-Ghaleh N, Giller K, Becker S, Zweckstetter M (2011) Biophys J 101:1202–1211

84. Yang DS, McLaurin J, Qin K, Westaway D, Fraser PE (2000) Eur J Biochem 267:6692–6698

85. Miura T, Suzuki K, Takeuchi H (2001) J Mol Struct 598:79–84

86. Curtain CC, Ali F, Volitakis I, Cherny RA, Norton RS, Beyreuther K, Barrow CJ, Masters CL, Bush AI, Barnham KJ (2001) J Biol Chem 276:20466–20473

87. Miura T, Suzuki K, Kohata N, Takeuchi H (2000) Biochemistry 39:7024–7031

88. Heise H (2008) ChemBioChem 9:179–189

89. Paravastu AK, Qahwash I, Leapman RD, Meredith SC, Tycko R (2009) Proc Natl Acad Sci USA 106:7443–7448

90. Spencer RG, Halverson KJ, Auger M, McDermott AE, Griffin RG, Lansbury PT Jr (1991) Biochemistry 30:10382–10387

91. Lansbury PT Jr, Costa PR, Griffiths JM, Simon EJ, Auger M, Halverson KJ, Kocisko DA, Hendsch ZS, Ashburn TT, Spencer RG et al (1995) Nat Struct Biol 2:990–998

92. Costa PR, Kocisko DA, Sun BQ, Lansbury PT Jr, Griffin RG (1997) J Am Chem Soc 119:10487–10493

93. Antzutkin ON, Balbach JJ, Leapman RD, Rizzo NW, Reed J, Tycko R (2000) Proc Natl Acad Sci USA 97:13045–13050

94. Benzinger TL, Gregory DM, Burkoth TS, Miller-Auer H, Lynn DG, Botto RE, Meredith SC (1998) Proc Natl Acad Sci USA 95:13407–13412

95. Lührs T, Ritter C, Adrian M, Riek-Loher D, Bohrmann B, Döbeli H, Schubert D, Riek R (2005) Proc Natl Acad Sci USA 102:17342–17347

96. Luo J, Otero JM, Yu CH, Wärmländer SK, Gräslund A, Overhand M, Abrahams JP (2013) Chemistry 19:17338–17348

97. Qiang W, Yau WM, Luo Y, Mattson MP, Tycko R (2012) Proc Natl Acad Sci USA 109:4443–4448

98. Lu JX, Qiang W, Yau WM, Schwieters CD, Meredith SC, Tycko R (2013) Cell 154:1257–1268

99. Safar J, Wille H, Itri V, Groth D, Serban H, Torchia M, Cohen FE, Prusiner SB (1998) Nat Med 4:1157–1165
100. Stohr J, Watts JC, Mensinger ZL, Oehler A, Grillo SK, DeArmond SJ, Prusiner SB, Giles K (2012) Proc Natl Acad Sci USA 109:11025–11030
101. Bertini I, Gallo G, Korsak M, Luchinat C, Mao J, Ravera E (2013) ChemBioChem 14:1891–1897
102. Parthasarathy S, Long F, Miller Y, Xiao Y, McElheny D, Thurber K, Ma B, Nussinov R, Ishii Y (2011) J Am Chem Soc 133:3390–3400
103. Grigorieff N, Harrison SC (2011) Curr Opin Struct Biol 21:265–273
104. Nederlof I, Li YW, van Heel M, Abrahams JP (2013) Acta Crystallogr Sect D Biol Crystallogr 69:852–859
105. Sachse C, Xu C, Wieligmann K, Diekmann S, Grigorieff N, Fändrich M (2006) J Mol Biol 362:347–354
106. Sachse C, Fändrich M, Grigorieff N (2008) Proc Natl Acad Sci USA 105:7462–7466
107. Sachse C, Grigorieff N, Fändrich M (2010) Angew Chem Int Ed Engl 49:1321–1323
108. Zhang R, Hu X, Khant H, Ludtke SJ, Chiu W, Schmid MF, Frieden C, Lee JM (2009) Proc Natl Acad Sci USA 106:4653–4658
109. Miller Y, Ma B, Tsai CJ, Nussinov R (2010) Proc Natl Acad Sci USA 107:14128–14133
110. Schmidt M, Sachse C, Richter W, Xu C, Fändrich M, Grigorieff N (2009) Proc Natl Acad Sci USA 106:19813–19818
111. Bodner CR, Dobson CM, Bax A (2009) J Mol Biol 390:775–790
112. Hallbeck M, Nath S, Marcusson J (2013) Neuroscientist 19:560–566
113. Matlack KE, Tardiff DF, Narayan P, Hamamichi S, Caldwell KA, Caldwell GA, Lindquist S (2014) Proc Natl Acad Sci USA 111:4013–4018
114. Petkova AT, Yau WM, Tycko R (2006) Biochemistry 45:498–512
115. Pettersen EF, Goddard TD, Huang CC, Couch GS, Greenblatt DM, Meng EC, Ferrin TE (2004) J Comput Chem 25:1605–1612